The Theory of Band Gaps in Nano-Porous Silicon Carbide

Colton J. Barger, Tyler C. Summers, Blair R. Tuttle, Andrew O'Hara, and Sokrates T. Pantelides

Pennsylvania State University: Erie, The Behrend College and

Vanderbilt University

(Dated: July 31, 2018)

Abstract

In an effort to characterize leakage currents in nano-porous silicon carbide alloys, we use first-principle methods to determine the magnitude of the band gap in many theoretical models. We create an analytical model that describes how defects added to nano-porous silicon carbide contribute to changing the magnitude of the band gap. In the end we show that creating hydrogenated pores leads to an increase in the band gap, but the addition of Si-Si bonds effectively lowers the magnitude of the band gap.

INTRODUCTION

Over the years, process node size in integrated circuit technology has decreased dramatically. Smaller process node size has allowed the manufacturing cost of integrated circuits to decrease, while performance remains the same, or even increases due to the lower driving voltage needed to activate the transistors. Additionally, lower voltage leads to decreased power consumption in these circuits. More recently, leakage currents caused by defects in insulating materials have been more of a concern. As process node size decreases, the defects causing leakage currents increase. When a device is switched on, the effects of leakage currents are felt in the time taken to charge a capacitor, or the delay time. As scaling of integrated circuits continues to go down, more interconnect is required and the effect of the delay time is increased.

In an effort to reduce the delay time in integrated circuit technology, low-k dielectrics such as silicon dioxide or porous silicon carbide have been used. The problem with these materials stems from the lack of understanding of the defects that cause leakage current.

In an effort to characterize some of the defects leading to leakage current, we study the band gaps of porous silicon carbide and the effects that added perturbations have on the band gap of these alloys. In this paper, we study several models of hydrogenated nano-porous silicon carbide and create an analytical model describing the band gap. In the future we will study defects and the energy levels they introduce in the band gap.

METHODS

We perform calculations using density functional theory as implemented in the Vienna Ab Initio Simulation Package (VASP) [1]. VASP is a computer program for modeling on the atomic scale by solving a Schrödinger-like equation numerically. We will be using density functional theory (DFT) to calculate the band gaps for models of nano-porous silicon carbide. These calculations will be done at the Gamma point in the Brillouin zone with a plane wave cutoff value of $E_{\text{cut}} = 400\text{eV}$. DFT determines the electron density and the electronic structure of the material. Using conjugate gradient minimization, VASP slightly moves the position of each atom in the material until the force between each atom is minimized. The stopping criterion for our process to end is that each atom feels a force less than $0.01\text{eV}/\text{Å}$.

Each model is constructed using a nano-pore-maker code made by students from Penn State

Behrend [3]. The code takes a VASP POSCAR file as input along with user-specified directions on where to put the nano-pore, the size of the nano-pore, and what element to passivate dangling bonds with. The code outputs a .vasp file with the specified nano-pore. More information on the nano-pore-maker code and how to use it can be found at `https://github.com/brt10/Nano-Pore-Maker`. An example of a model we will study is given in Fig. 1. We are starting from supercells of 3C-SiC to create our models. In the model shown we have created a nano-pore in the 3C-SiC crystal structure, passivating dangling bonds with hydrogens. Each hydrogen (white) is bonded to a carbon atom (brown). The length of the square supercell is approximately 13Å, for reference.

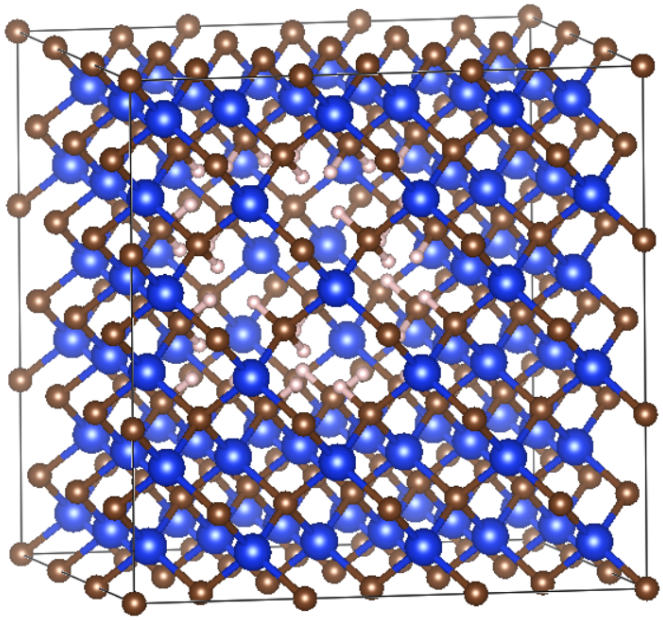

Figure 1. An example ball and stick figure of a system that we will be studying. The blue balls are silicon atoms, brown are carbons, and white atoms are hydrogens. The gray lines represent the edges of the SiC unit cell.

We develop an analytical model to describe the band gaps of our results. In the spirit of first-order perturbation theory, we fit the band gap results to the equation

$$E_{\mathrm{g}}^{\mathrm{model}} = E_{\mathrm{g}}^{\mathrm{SiC}} + \sum_i n_i \Delta E_{\mathrm{g}}^{i} + n_{\mathrm{SiC}}^{*} \Delta E_{\mathrm{g}}^{\mathrm{SiC}} \tag{1}$$

where $E_{\mathrm{g}}^{\mathrm{model}}$ is the energy gap of our models and $E_{\mathrm{g}}^{\mathrm{SiC}}$ is the energy gap of the crystalline 3C-SiC. The i in the summation represents perturbations made to the original 3C-SiC crystalline structure. For example, during the creation of the nano-pore in Fig. 1 bonds between carbon atoms and

hydrogen atoms are created which are not in the original model. The part of the summation created by this would be $n_{\mathrm{CH}}\Delta E_{\mathrm{g}}^{\mathrm{CH}}$, where n_{CH} is the ratio of the bond density of C-H bonds in the model to the bond density of Si-C bonds in the 3C-SiC structure, and $\Delta E_{\mathrm{g}}^{\mathrm{CH}}$ is the change in the energy gap that the C-H bonds contribute to the original model. The n_{SiC}^{*} variable is equivalent to $1 - n_{\mathrm{SiC}}$ in order for our analytical model to describe how the loss of Si-C bonds contribute to the band gap. Valid bonds for the models we observe include Si-C, C-H, Si-H, Si-Si, and C-C bonds.

We will try to solve for the unknown parameters in Eq. (1) using different statistical methods with many models. One method is to create models with just C-H bonds or just Si-H bonds to create systems where $\Delta E_{\mathrm{g}}^{\mathrm{SiH}}$ or $\Delta E_{\mathrm{g}}^{\mathrm{CH}}$ are canceled out, respectively. This allows us to solve for the unknown parameters by solving systems of equations. Another method of solving for the unknown parameters is by using multiple linear regression techniques. This method allows us to make a surface of best-fit in higher dimensions to fit the data. This technique reduces errors made in other techniques that depend on trial and error.

We would expect to see the value of $\Delta E_{\mathrm{g}}^{\mathrm{CH}}$ be positive according to physical experiments done by Pomorski *et al.* in [2]. In this study n_{CH} is a measure of how many hydrogens were added to the system. In [2] we see that the more hydrogenated silicon carbide is, the higher the band gap should be up to a point. Similarly, we should see that $\Delta E_{\mathrm{g}}^{\mathrm{SiC}}$ is positive as well. n_{SiC}^{*} is a measure of many how Si-C bonds were removed to create more C-H bonds. This should be positive, as adding hydrogen to the system increases the size of the band gap.

RESULTS

Results reported in this section are properties of the material that can be measured through experimental means. Results include bond densities (measurable through Fourier transform infrared spectroscopy), band gaps, densities, and atomic compositions. In addition to these measurable quantities we have also included the derived quantities which will be of use in Eq. (1).

C-H Bonds

We begin our study by looking at the simplest of models that involve only the addition of C-H bonds through removal of Si-C bonds. To solve for the fitting parameters $\Delta E_{\mathrm{g}}^{\mathrm{SiC}}$ and $\Delta E_{\mathrm{g}}^{\mathrm{CH}}$ in Eq. (1) we will need to create at least two models of varying hydrogen content and calculate their

Models	Bond Densities (10^{21}cm^{-3})		Gap (eV)	ρ (g/cm^3)	Atomic %		
	Si-C	C-H			Si	C	H
Crystalline	193.0	0.00	1.35	3.21	50	50	0
4H	191.3	1.79	1.40	3.20	48.9	49.3	1.8
12H_1	185.9	5.36	1.50	3.13	46.6	48.0	5.4
24H_2	178.7	10.72	1.66	3.05	43.5	46.1	10.4
36H_3	171.6	16.09	1.78	2.96	40.5	44.3	15.2
28H	175.2	12.51	1.63	3.00	42.4	45.5	12.1
36H	169.8	16.09	1.75	2.93	40.4	44.3	15.3
56H	151.9	25.02	1.99	2.70	35.4	41.3	23.3
72H	150.1	32.17	2.16	2.71	32.6	39.5	27.9
84H	143.0	37.54	2.19	2.63	30.2	38.1	31.7
108H	128.7	48.26	2.46	2.46	25.8	35.5	38.7

Table I. Data from the DFT calculations for each model with C-H bonds. Shown are the Si-C and C-H bond densities in 10^{21}cm^{-3}, the band gap in eV, the theoretical density of the material, and the atomic composition in percentage.

respective bond densities using VASP. We create many different models ranging from 1.83% to 38.7% hydrogen content. Shown in Table I and Table II are the calculated data for each of our theoretical models. We will analyze these results in the later analysis section.

The naming scheme of the models shown in Table I and Table II comes from the number of hydrogens added to the model after the creation of the nano-pore. The 4H model would have four hydrogen atoms in the supercell, for example.

From the results in Table I we see that, in general, the band gap tends to increase as more hydrogens and nano-pores are added. The band gaps also seem to increase linearly as the C-H bond density increases and the Si-C bond density decreases. The densities of the models also decrease as more hydrogens are added. This is expected, as hydrogens are added to the models as replacements for the silicons and carbons that are removed.

Models	$n^*_{SiC} \times 10^{-3}$	$n_{CH} \times 10^{-3}$
Crystalline	0	0
4H	9.26	9.26
12H_1	37.0	27.8
24H_2	74.1	55.6
36H_3	111	83.3
28H	92.6	64.8
36H	120	83.3
56H	213	130
72H	222	167
84H	259	194
108H	333	250

Table II. The n^*_{SiC} and n_{CH} values for each model, derived from the bond densities found in Table I.

Mixed C-H and Si-H Bonds

After looking at models where we have isolated both C-H and Si-H bonds along with Si-C bonding, we look at models where we have both types of bonding in addition to the Si-C bonding in nanoporous silicon carbide. We create many models with varying C-H and Si-H bond densities. The results from the DFT calculations are reported in Table III.

The naming mechanism used for the mixed C-H and Si-H models reported in Table III are the same as the C-H models in the previous section. The numbers represent the amount of hydrogen added to the model after the cretion of a nano-pore in crystalline 3C-SiC. The general trend for the band gap is to increase as more pores are created. There seems to be a negative correlation between the Si-C bond density and the band gap, while the C-H and Si-H generally have a positive correlation with the band gap.

Si-Si Bonds

Information for models with Si-Si bonds is not reported due to large amounts of data. The analysis for these models can be found in the Analysis section.

Models	Bond Densities (10^{21}cm^{-3})			Gap (eV)	ρ (g/cm^3)	Atomic %		
	Si-C	C-H	Si-H	1.35		Si	C	H
Crystalline	193.0	0.00	0.00	1.35	3.21	50.0	50.0	0.0
14H	180.4	1.31	4.81	1.43	3.08	47.3	46.4	6.3
24H	173.3	5.20	5.20	1.51	2.99	44.8	44.8	10.4
28H	165.3	6.06	6.06	1.54	2.87	43.8	43.8	12.4
34H	159.4	9.93	4.75	1.68	2.78	41.9	43.2	15.0
42H	152.6	9.83	8.12	1.73	2.71	40.7	41.1	18.2
46H	147.8	12.36	7.24	1.84	2.64	39.4	40.7	19.9
52H	141.8	11.82	10.13	1.87	2.57	38.6	39.1	22.3
60H	135.8	15.09	10.06	1.96	2.50	36.7	38.0	25.3
64H	130.9	14.18	12.51	2.04	2.44	36.3	36.7	27.0
64H_2	129.0	14.15	12.46	2.05	2.41	36.2	36.6	27.2
68H	124.0	13.23	14.89	2.00	2.35	35.7	35.3	28.9
72H	119.9	13.14	16.43	2.07	2.30	35.2	34.3	30.5
76H	115.0	12.24	18.76	2.27	2.25	34.7	33.1	32.2
84H	108.9	12.10	21.78	2.33	2.18	33.8	31.3	35.0
88H	103.8	11.18	23.96	2.27	2.12	33.3	30.0	36.7
92H	100.2	10.42	26.46	2.48	2.09	32.9	28.8	38.3

Table III. Results from the DFT calculations for the models with mixed C-H and Si-H bonding.

ANALYSIS

C-H Bond Model Analysis

Beginning to analyze the C-H models studied, Eq. (1) will now be

$$E_{\rm g}^{\rm model} = E_{\rm g}^{\rm SiC} + n_{\rm SiC}^{*}\Delta E_{\rm g}^{\rm SiC} + n_{\rm CH}\Delta E_{\rm g}^{\rm CH} \tag{2}$$

due to the fact that there are no Si-H bonds in the models being studied in this section.

Since Table I suggests that there may be a linear correlation between the C-H bond density and the band gap, we start by looking at a way to predict the band gaps of our models using the C-H bond density. We plot the DFT gap as a function of C-H bond density. In Fig. 2 we see a high

Models	DFT Gap	C-H Density Prediction	Linear Regression Model
Crystalline	1.35	1.39	1.35
4H	1.40	1.43	1.38
12H_1	1.50	1.51	1.47
24H_2	1.66	1.63	1.59
36H_3	1.78	1.75	1.71
28H	1.63	1.67	1.64
36H	1.75	1.75	1.72
56H	1.99	1.95	1.96
72H	2.16	2.12	2.08
84H	2.19	2.24	2.21
108H	2.46	2.46	2.45
RMSE (%)		0.033 eV (1.86%)	0.041 eV (2.24%)

Table IV. Predictions for the band gaps of the C-H models in eV. The band gap calculated from DFT is given in the second column, C-H bond density model prediction and linear regression model band gaps in columns three and four, respectively. The root mean square error in eV and percentage for both of the models are given in the last row.

linear correlation with a coefficient of determination of $R^2 = 0.99205$ and a root mean square error of only 0.033 eV. This agrees with the physical experiments done by Pomorski *et al.* in [2].

In a further attempt to get more accurate values for ΔE_g^{SiC} and ΔE_g^{CH}, we plot the band energy as a function of n^*_{SiC} and n_{CH} and find a best-fit plane in three dimensions. A sample plot of this can be seen in Fig. 3. From the plane of best fit, we get that $\Delta E_g^{SiC} = 0.981$ and $\Delta E_g^{CH} = 3.111$. Using these values in Eq. (2) we can get accurate predictions for the band gaps for our models. These predictions are reported in Table IV along with the predictions from the other model and the root mean square error. A plot of the band gap predictions using these values versus the band gap from the DFT calculations is shown in Fig. 4.

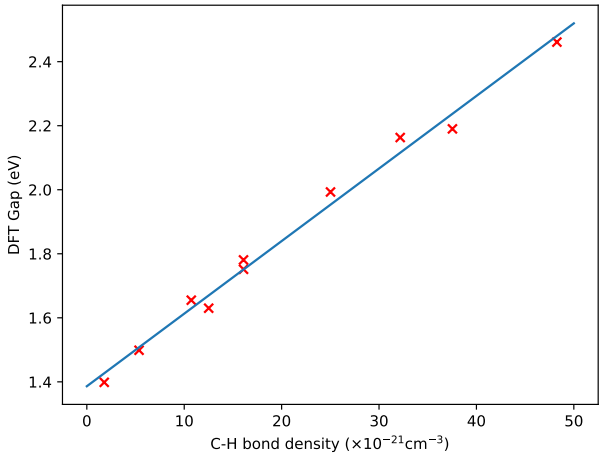

Figure 2. The DFT gap as a function of C-H bond density. The standard error from the line of best fit is approximately 0.033 eV and 1.86%.

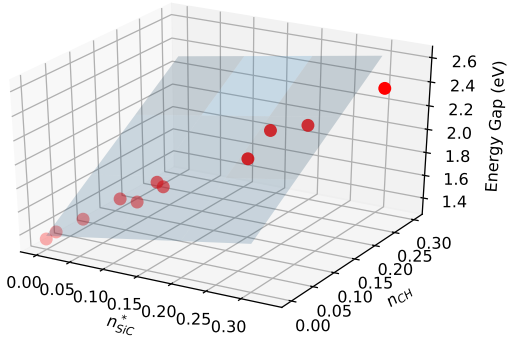

Figure 3. A graph of the energy gap as a function of n^*_{SiC} and n_{CH}.

Mixed Bonding Analysis

To begin studying the mixed C-H and Si-H bonding models, we start by using $\Delta E_{\mathrm{g}}^{\mathrm{SiC}} = 0.981$ and $\Delta E_{\mathrm{g}}^{\mathrm{CH}} = 3.111$ from the C-H models in Eq. (1). With those values being used in Eq. (1), the only unknown parameter to solve for is $\Delta E_{\mathrm{g}}^{\mathrm{SiH}}$. This unknown parameter can be solved for to reduce error with a linear regression analysis with the y-intercept fixed at 1.35, or the band gap of the crystalline model. We do this to see if we can obtain a comprehensive analytical model that applies to all of our systems.

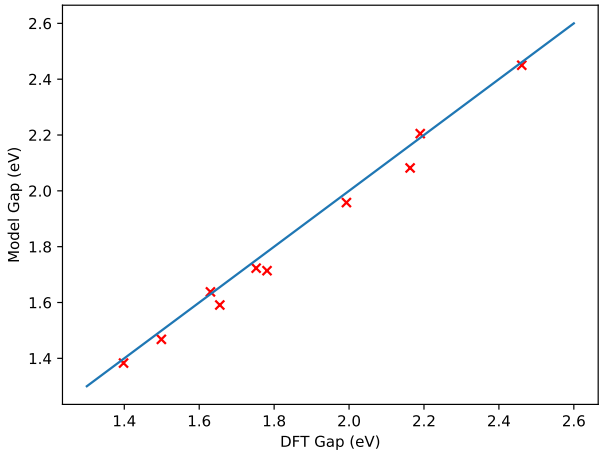

Figure 4. A plot of band gap calculated using DFT versus the band gap predicted using the plane of best-fit. The root mean square error is 0.034eV and 1.81%.

Through linear regression, we find that the unknown parameter $\Delta E_{\mathrm{g}}^{\mathrm{SiH}} = 2.51$ for this specific model. With all three unknowns in Eq. (1) accounted for, we are able to make predictions for all of our models based off of this analytic model. The predictions for the band gaps for all of the mixed C-H and Si-H models can be found in Table V. A plot of the band gap calculated using DFT versus the analytic model band gap can be see in Fig. 5.

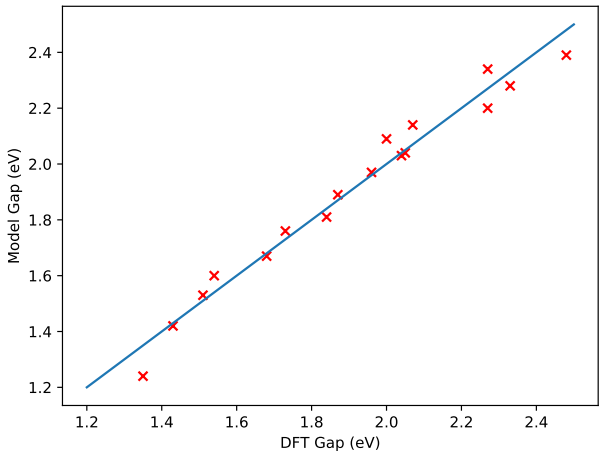

Figure 5. A scatter plot of the band gap of the mixed C-H and Si-H bond models predicted using the C-H model parameters, plus the new n_{SiH} parameter calculated from a linear fit, versus the band gap calculated using DFT. The blue line shown is the line of equality. The root mean square error is 0.054eV and 3.4%.

Models	DFT Gap	C-H Model	Linear Regression Model
Crystalline	1.35	1.35	1.35
14H	1.43	1.49	1.50
24H	1.51	1.60	1.58
28H	1.54	1.66	1.67
34H	1.68	1.74	1.72
42H	1.73	1.82	1.81
46H	1.84	1.87	1.86
52H	1.87	1.93	1.94
60H	1.96	2.01	2.00
64H	2.04	2.05	2.07
64H_2	2.05	2.06	2.09
68H	2.00	2.10	2.15
72H	2.07	2.14	2.20
76H	2.27	2.18	2.27
84H	2.33	2.25	2.35
88H	2.27	2.29	2.41
92H	2.48	2.33	2.47
RMSE (%)		0.075 eV (4.6%)	0.079 eV (4.9%)

Table V. Predictions for the band gaps of the mixed C-H and Si-H bonding models in eV. The second column gives the gap calculated using DFT, the third column gives the band gap prediction from the analytical model involving the C-H model parameters, and the fourth column gives the band gap prediction from the multiple linear regression analytical model. Also given in the last row are each analytical model's root mean square error in both eV and percentage.

Similar to what we did with the C-H models, we perform a multiple linear regression analysis on the band gap to fit it as a function of n^*_{SiC}, n_{CH}, and n_{SiH} on a surface in higher dimensions. This will allow us to solve for the three unknown parameters, $\Delta E_{\mathrm{g}}^{\mathrm{SiC}}$, $\Delta E_{\mathrm{g}}^{\mathrm{CH}}$, and $\Delta E_{\mathrm{g}}^{\mathrm{SiH}}$, independently of the results seen in the C-H models section.

With the multiple linear regression, we can find that $\Delta E_{\mathrm{g}}^{\mathrm{SiC}} = 1.994$, $\Delta E_{\mathrm{g}}^{\mathrm{CH}} = 0.039$, and

$\Delta E_g^{SiH} = 1.163$. Using these values for the parameters in Eq. (1) we can predict the band gaps using this new analytic model. The results of this predictive model can be seen in Table V along with the model's error and the other analytic model described earlier in this section.A plot of the band gap calculated using DFT versus the analytic model band gap can be see in Fig. 6.

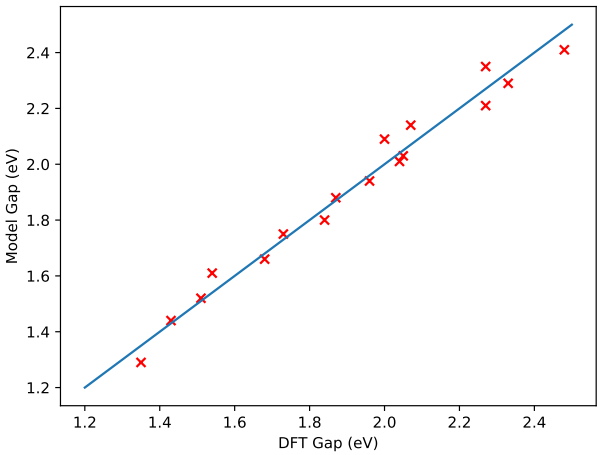

Figure 6. A plot of the band gap of the mixed C-H and Si-H models predicted using the parameters from multiple linear regression versus the band gap calculated using DFT. The blue line shown is the line of equality. The root mean square error is 0.051eV and 3.05%.

Si-Si Bonds

With the addition of Si-Si bonds into our nano-porous silicon carbide models, we hypothesize that the band gaps of our structures will go down, as crystalline silicon has a lower experimental band gap (1.1eV) than crystalline silicon carbide (2.36eV).

Eq. (1) will now take on the form

$$E_g^{model} = E_g^{SiC} + n_{SiC}^{*}\Delta E_g^{SiC} + n_{CH}\Delta E_g^{CH} + n_{SiH}\Delta E_g^{SiH} + n_{SiSi}\Delta E_g^{SiSi} \tag{3}$$

with the addition of Si-Si bonds.

Creation of the Si-Si bond models was done through manipulation of some of the Mixed C-H and Si-H bond models. Algorithms were created that allow for the switching of carbon atoms and silicon atoms to create Si-Si bonds at the surface of nano-pores. The created structures were allowed to relax using VASP, and the band gaps were analyzed to create a model through linear

regression. The model's gap as a function of the gaps found using DFT are seen in Fig. 7. We report fitting parameters of $\Delta E_g^{SiC} = 0.95$, $\Delta E_g^{CH} = 2.98$, $\Delta E_g^{SiH} = 0.78$, and $\Delta E_g^{SiSi} = -10.9$. As expected, the addition of Si-Si bonds seems to decrease the band gap of our models by a significant margin as indicated by the negative value of ΔE_g^{SiSi}.

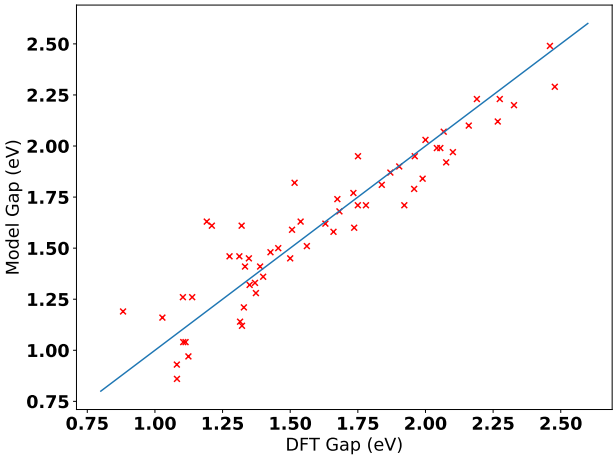

Figure 7. The band gaps found using a linear model as a function of the band gaps found using DFT. Red crosses represent each data point, and the blue lines serves as the line of equality between data, or the ideal fit. The mean absolute deviation of these models is approximately 0.1 eV

It can be seen that there are some outliers that are far away from the blue line of equality in Fig. 7. We believe that the discrepancies between the measured band gap and the band gap predicted using our model can be explained through the clustering of silicon atoms. In Fig. 8 we illustrate how the addition of one silicon atom in the place of a carbon atom can change the bonding topology of our system dramatically, which can lead to a big change in the band gap.

Presently, we are working on algorithms to quantify the bonding topology of these silicon clusters and incorporate them into our general model for the band gap of nano-porous silicon carbide alloys.

CONCLUSION

We have created an analytic model that can be used for predicting the band gaps in nano-porous silicon carbide. Though imperfect for models incorporating Si-Si bonding, we have identified

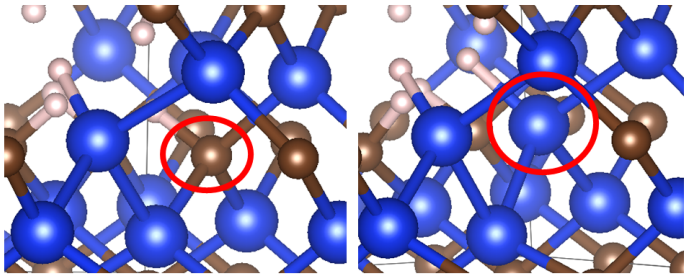

$E_g = 1.87\ eV$ $E_g = 1.42\ eV$

Figure 8. A figure explaining the possible defect that leads to large changes in the band gap of nano-porous silicon carbide. The circled carbon atom on the left was replaced with the circled silicon atom on the right, and the band gap decreased by 0.45 eV. By replacing the carbon with a silicon atom, a cluster of seven silicon atoms was formed, forming a network of just silicon. In the system on the left, there is only a single cluster of four connected silicon atoms. By changing one carbon atom to a silicon, the possible cluster sizes of silicon atoms can vary greatly.

silicon clustering as a defect leading the increased variability of band gaps and are working to incorporate this into our model.

Additionally, we hope to analyze the same models presented in this paper using a new DFT hybridization functional that gives more accurate band gaps represented in experimental studies.

SUPPLEMENTAL RESULTS

Si-H Bonds

Like we did with isolating C-H bonding defects in our models, we created additional models where we isolate S-H bonds. These models were not included in the final analysis, so we will not analyze these models, as they form bonds that are not physical during the VASP calculations. A hydrogenated carbon vacancy proves to be too small for three hydrogen atoms. With the PBE functional, the three carbon atoms repel each other strongly during the relaxation of the crystal, and this ends with the formation of Si-H-Si bonds, which are not physical in the systems we

hope to apply our analytical model to. Preliminary results lead us to believe that this behavior is functional-dependent. Using a new hydridization functional we have witnessed these same systems relaxing to a more viable configuration. The results from the PBE calculations can be found in Table VI.

Models	**DFT Gap (eV)**	**% H**	n^*_{SiC} ($\times 10^3$)	n_{SiH}($\times 10^3$)
12H_1	1.37	5.38	37.0	27.8
24H_2	1.42	10.4	74.1	55.6
36H_3	1.44	15.2	111.1	83.3
40H	1.56	17.0	138.9	92.6
44H	1.59	18.7	166.7	101.9
48H	1.57	20.2	175.9	111.1
56H	1.71	23.1	203.7	129.6
60H	1.69	24.9	231.5	138.9
64H	1.74	26.7	259.3	148.1
68H	1.70	28.0	268.5	157.4
76H	1.85	31.0	305.6	175.9
Crystalline	1.35	0	0	0

Table VI. The table above shows data for the models in this portion of the study. The numbers again represent the number of hydrogen atoms in the model, and the underscores are to differentiate the models from one another. Data given in the table is the DFT gap, model gap, percent hydrogen, n^*_{SiC}, and n_{SiH}.

ACKNOWLEDGEMENTS

We would like to thank Vanderbilt's 2018 Summer REU for integrating Colton into their program. This research was conducted usign Advanced CyberInfrastructure computational resources provided by the Institute of Cyberscience at The Pennsylvania State University (https://ics.psu.edu/).

[1] G. Kresse and J. Furthmüller. Efficient iterative schemes for ab initio total-energy calculations using a plane-wave basis set. *Phys. Rev. B*, 54:11169–11186, Oct 1996.

[2] T.A. Pomorski, B.C. Bittel, C.J. Cochrane, P.M. Lenahan, J. Bielefeld, and S.W. King. Defects and electronic transport in hydrogenated amorphous sic films of interest for low dielectric constant back end of the line dielectric systems. *Journal of Applied Physics*, 114(2), 2013.

[3] Blair R. Tuttle. Nano-pore-maker. `https://github.com/brt10/Nano-Pore-Maker`, 2017.